nature physics

LETTERS

https://doi.org/10.1038/s41567-022-01614-y

Check for updates

OPEN

Observation of an exotic narrow doubly charmed tetraquark

LHCb Collaboration*

Conventional, hadronic matter consists of baryons and mesons made of three quarks and a quark–antiquark pair, respectively[1,2]. Here, we report the observation of a hadronic state containing four quarks in the Large Hadron Collider beauty experiment. This so-called tetraquark contains two charm quarks, a $\bar{u}$ and a $\bar{d}$ quark. This exotic state has a mass of approximately 3,875 MeV and manifests as a narrow peak in the mass spectrum of $D^0D^0\pi^+$ mesons just below the $D^{*+}D^0$ mass threshold. The near-threshold mass together with the narrow width reveals the resonance nature of the state.

Quantum chromodynamics, the theory of the strong force, describes the interactions of coloured quarks and gluons and the formation of hadronic matter, that is, mesons and baryons. While quantum chromodynamics makes precise predictions at high energies, the theory has difficulties describing the interactions of quarks in hadrons from first principles due to the highly nonperturbative regime at the corresponding energy scale. Hence, the field of hadron spectroscopy is driven by experimental discoveries that are sometimes unexpected, which could lead to changes in the research landscape. Along with conventional mesons and baryons, made of a quark–antiquark pair ($q_1\bar{q}_2$) and three quarks ($q_1q_2q_3$), respectively, particles with an alternative quark content, known as exotic states, have been actively discussed since the birth of the constituent quark model[1–8]. This discussion has been revived by recent observations of numerous tetraquark $q_1q_2\bar{q}_3\bar{q}_4$ and pentaquark $q_1q_2q_3q_4\bar{q}_5$ candidates[9–36]. Due to the closeness of their masses to known particle-pair thresholds[37,38], many of these states are likely to be hadronic molecules[39–42] where colour-singlet hadrons are bound by residual nuclear forces similar to the electromagnetic van der Waals forces attracting electrically neutral atoms and molecules. An ordinary example of a hadronic molecule is the deuteron formed by a proton and a neutron. On the other hand, an interpretation of exotic states as compact multiquark structures is also possible[43].

All exotic hadrons observed so far predominantly decay via the strong interaction, and their decay widths vary from a few to a few hundred MeV. A discovery of a long-lived exotic state, stable with respect to the strong interaction, would be intriguing. A hadron with two heavy quarks Q and two light antiquarks $\bar{q}$, that is, $Q_1Q_2\bar{q}_1\bar{q}_2$, is a prime candidate to form such a state[44–49]. In the limit of a large heavy-quark mass, the two heavy quarks Q_1Q_2 form a point-like, heavy, colour-antitriplet object that behaves similarly to an antiquark, and the corresponding state should be bound. It is expected that the b quark is heavy enough to sustain the existence of a stable $bb\bar{u}\bar{d}$ state with a binding energy of about 200 MeV with respect to the sum of the masses of the pseudoscalar, B^- or $\overline{B}^0$, and vector, B^{*-} or $\overline{B}^{*0}$, beauty mesons, which defines the minimal mass for the strong decay to be allowed. In the case of the $bc\bar{u}\bar{d}$ and $cc\bar{u}\bar{d}$ systems, there is currently no consensus regarding whether such states exist and are narrow enough to be detected experimentally. The similarity of the $cc\bar{u}\bar{d}$ tetraquark state and the Ξ_{cc}^{++} baryon containing two c quarks and a u quark leads to a relationship between the properties of the two states. In particular, the measured mass of the Ξ_{cc}^{++} baryon with quark content ccu[50–52] implies that the mass of the $cc\bar{u}\bar{d}$ tetraquark is close to the sum of the masses of the D^0 and D^{*+} mesons with quark content of $c\bar{u}$ and $c\bar{d}$, respectively, as suggested in ref. [53]. Theoretical predictions for the mass of the $cc\bar{u}\bar{d}$ ground state with spin-parity quantum numbers $J^P = 1^+$ and isospin $I = 0$, denoted hereafter as T_{cc}^+, relative to the $D^{*+}D^0$ mass threshold

$$\delta m \equiv m_{T_{cc}^+} - (m_{D^{*+}} + m_{D^0}) \tag{1}$$

lie in the range of $-300 < \delta m < 300$ MeV (refs. [53–84]), where $m_{D^{*+}}$ and m_{D^0} denote the known masses of the D^{*+} and D^0 mesons[38]. Lattice quantum chromodynamics calculations also do not provide a definite conclusion on the existence of the T_{cc}^+ state or its binding energy[73,85–87]. The observation of the Ξ_{cc}^{++} baryon[50,51] and of a new exotic resonance decaying to a pair of J/ψ mesons[29] by the LHCb experiment motivates the search for the T_{cc}^+ state.

In this Letter, the observation of a narrow state in the $D^0D^0\pi^+$ mass spectrum near the $D^{*+}D^0$ mass threshold compatible with being a T_{cc}^+ tetraquark state is reported. Throughout this Letter, charge conjugate decays are implied. The study is based on proton–proton (pp) collision data collected by the LHCb detector at the Large Hadron Collider at the European Organization for Nuclear Research at centre-of-mass energies of 7, 8 and 13 TeV, corresponding to integrated luminosity of 9 fb^{-1}. The LHCb detector[88,89] is a single-arm forward spectrometer covering the pseudorapidity range of $2 < \eta < 5$, designed to study particles containing b or c quarks and is further described in Methods. The pseudorapidity η is defined as $-\log\left(\tan\frac{\theta}{2}\right)$, where θ is a polar angle of the track relative to the proton beam line.

The $D^0D^0\pi^+$ final state is reconstructed by selecting events with two D^0 mesons and a positively charged pion, all produced at the same pp interaction point. Both D^0 mesons are reconstructed in the $D^0 \to K^-\pi^+$ decay channel. The selection criteria are similar to those used in ref. [90]. To subtract the background not originating from two D^0 candidates, an extended, unbinned maximum-likelihood fit to the two-dimensional distribution of the masses of the two D^0 candidates is performed. The corresponding procedure, together with the selection criteria, is described in detail in Methods. To improve the δm mass resolution and to make the determination insensitive to the precision of the D^0 meson mass, the mass of the $D^0D^0\pi^+$ combinations is calculated with the mass of each D^0 meson constrained to the known value[38]. The resulting $D^0D^0\pi^+$ mass distribution for selected $D^0D^0\pi^+$ combinations is shown in Fig. 1. A narrow peak near the $D^{*+}D^0$ mass threshold is clearly visible.

An extended, unbinned, maximum-likelihood fit to the $D^0D^0\pi^+$ mass distribution is performed using a model consisting of the signal

*A list of authors and their affiliations appears online.

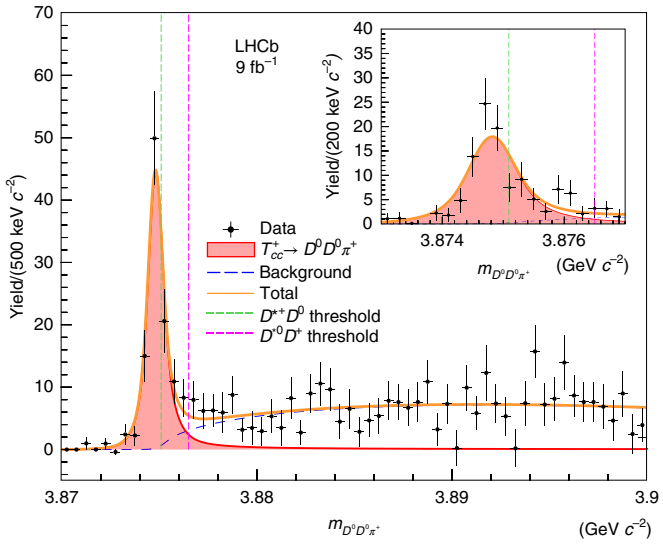

Fig. 1 | The distribution of the $D^0D^0\pi^+$ mass. The distribution of the $D^0D^0\pi^+$ mass after statistical subtraction of the contribution of the non-D^0 background, with the result of the fit with the two-component function described in the text. The horizontal bin width is indicated on the vertical axis legend. The inset shows a zoomed signal region with a fine binning scheme. Uncertainties on the data points are statistical only and represent one standard deviation, calculated as a sum in quadrature of the assigned weights from the background subtraction procedure.

Table 1 | Parameters obtained from the fit to the $D^0D^0\pi^+$ mass spectrum: signal yield, N, BW mass relative to the $D^{*+}D^0$ mass threshold, $\delta m_{\rm BW}$, and width, $\Gamma_{\rm BW}$. The uncertainties are statistical only

Parameter	Value
N	117 ± 16
$\delta m_{\rm BW}$	$-273 \pm 61\,{\rm keV}\,c^{-2}$
$\Gamma_{\rm BW}$	$410 \pm 165\,{\rm keV}$

Table 2 | Systematic uncertainties for the $\delta m_{\rm BW}$ and $\Gamma_{\rm BW}$ parameters. The total uncertainty is calculated as the sum in quadrature of all components except for those related to the assignment of $J^{\rm P}$ quantum numbers, which are handled separately

Source	$\sigma_{\delta m_{\rm BW}}$ (keV c^{-2})	$\sigma_{\Gamma_{\rm BW}}$ (keV)
Fit model		
Resolution model	2	7
Resolution correction factor	1	30
Background model	3	30
Model parameters	<1	<1
Momentum scale	3	—
Energy loss corrections	1	—
$D^{*+}-D^0$ mass difference	2	—
Total	5	43
$J^{\rm P}$ quantum numbers	$^{+11}_{-14}$	$^{+18}_{-38}$

and background components. The signal component is described by the convolution of the detector resolution with a resonant shape, which is modelled by a relativistic P-wave two-body Breit–Wigner (BW) function modified by a Blatt–Weisskopf form factor with a meson radius parameter of $3.5\,{\rm GeV}^{-1}$. The use of a P-wave resonance is motivated by the expected $J^{\rm P}=1^+$ quantum numbers for the T_{cc}^+ state. A two-body decay structure $T_{cc}^+ \to AB$ is assumed with $m_A = 2m_{D^0}$ and $m_B = m_{\pi^+}$, where m_{π^+} stands for the known mass of the π^+ meson. Several alternative prescriptions are used for the evaluation of the systematic uncertainties. Despite its simplicity, the model serves well to quantify the existence of the T_{cc}^+ state and to measure its properties, such as the position and the width of the resonance. A follow-up study[91] investigates the underlying nature of the T_{cc}^+ state, expanding on the modelling of the signal shape and the determination of its physical properties. The detector resolution is modelled by the sum of two Gaussian functions with a common mean, where the additional parameters are taken from simulation (Methods) with corrections applied[32,92,93]. The root mean square of the resolution function is around 400 keV c^{-2}. A study of the $D^0\pi^+$ mass distribution for $D^0D^0\pi^+$ combinations in the region above the $D^{*0}D^+$ mass threshold but below $3.9\,{\rm GeV}\,c^{-2}$ shows that approximately 90% of all random $D^0D^0\pi^+$ combinations contain a genuine D^{*+} meson. On the basis of this observation, the background component is parameterized by the product of a two-body phase space function and a positive second-order polynomial. The resulting function is convolved with the detector resolution.

The fit results are shown in Fig. 1, and the parameters of interest, namely the signal yield, N, the mass parameter of the BW function relative to the $D^{*+}D^0$ mass threshold, $\delta m_{\rm BW} \equiv m_{\rm BW} - (m_{D^{*+}} + m_{D^0})$, and the width parameter, $\Gamma_{\rm BW}$, are listed in Table 1. The statistical significance of the observed $T_{cc}^+D^0D^0\pi^+$ signal is estimated using Wilks' theorem to be 22 s.d. The fit suggests that the mass parameter of the BW shape is slightly below the $D^{*+}D^0$ mass threshold. The statistical significance of the hypothesis $\delta m_{\rm BW} < 0$ is estimated to be 4.3 s.d.

To validate the presence of the signal component, several additional cross-checks are performed. The data are categorized according to data-taking periods, including the polarity of the LHCb dipole magnet and the charge of the T_{cc}^+ candidates. Instead of statistically subtracting the non-D^0 background, the mass of each $D \to K^-\pi^+$ candidate is required to be within a narrow region around the known mass of the D^0 meson[38]. The results are found to be consistent among all samples and analysis techniques. Furthermore, dedicated studies are performed to ensure that the observed signal is not caused by kaon or pion misidentification, doubly Cabibbo-suppressed $D^0 \to K^+\pi^-$ decays or $D^0\overline{D}^0$ oscillations, decays of charm hadrons originating from beauty hadrons or artefacts due to the track reconstruction creating duplicate tracks.

Systematic uncertainties for the $\delta m_{\rm BW}$ and $\Gamma_{\rm BW}$ parameters are summarized in Table 2 and described below. The largest systematic uncertainty is related to the fit model and is studied using pseudo-experiments with alternative parameterizations of the $D^0D^0\pi^+$ mass shape. Several variations in the fit model are considered: changes in the signal model due to the imperfect knowledge of the detector resolution, an uncertainty in the correction factor for the resolution taken from control channels, parameterization of the background component and the additional model parameters of the BW function. The model uncertainty related to the assumption of $J^{\rm P}=1^+$ quantum numbers of the state is estimated and listed separately. The results are affected by the overall detector momentum scale, which is known to a relative precision of $\delta\alpha = 3\times10^{-4}$ (ref. [94]). The corresponding uncertainty is estimated using simulated samples where the momentum scale is modified by factors of $(1 \pm \delta\alpha)$. In the reconstruction, the momenta of charged tracks are corrected for energy loss in the detector material, the amount of which is known with a relative uncertainty of 10%. The resulting uncertainty

is assessed by varying the energy loss correction by ±10%. As the mass of the $D^0D^0\pi^+$ combinations is calculated with the mass of each D^0 meson constrained to the known value of the D^0 mass, the $\delta m_{\rm BW}$ parameter is insensitive to the precision of the D^0 mass. However, the small uncertainty of 2 keV c^{-2} for the $D^{*+}-D^0$ mass difference[38] directly affects the $\delta m_{\rm BW}$ value. The corresponding systematic uncertainty is added.

In summary, using the full dataset corresponding to an integrated luminosity of 9 fb^{-1} collected by the LHCb experiment at centre-of-mass energies of 7, 8 and 13 TeV, a narrow peak is observed in the mass spectrum of $D^0D^0\pi^+$ candidates produced promptly in pp collisions. The statistical significance of the peak is overwhelming. Using the BW parameterization, the location of the peak relative to the $D^{*+}D^0$ mass threshold, $\delta m_{\rm BW}$, and the width, $\Gamma_{\rm BW}$, are determined to be

$$\delta m_{\rm BW} = -273 \pm 61 \pm 5\,^{+11}_{-14}\,\text{keV}\,c^{-2},$$
$$\Gamma_{\rm BW} = 410 \pm 165 \pm 43\,^{+18}_{-38}\,\text{keV},$$

where the first uncertainty is statistical, the second is systematic and the third is related to the assignment of the $J^{\rm P}$ quantum numbers. The measured $\delta m_{\rm BW}$ value corresponds to a mass of approximately 3,875 MeV. This is the narrowest exotic state observed to date[37,38]. The minimal quark content for this state is $cc\bar{u}\bar{d}$. Two heavy quarks of the same flavour make it manifestly exotic, that is, beyond the conventional pattern of hadron formation found in mesons and baryons. Moreover, the combination of the near-threshold mass, narrow decay width and its appearance in prompt hadroproduction demonstrates its genuine resonance nature. The measured mass and width are consistent with the expected values for a T_{cc}^+ isoscalar tetraquark ground state with quantum numbers $J^{\rm P}=1^+$. The precision of the mass measurement with respect to the corresponding threshold is superior to those of all other exotic states, which will give better understanding of the nature of exotic states. A dedicated study of the reaction amplitudes for the $T_{cc}^+ \to D^0D^0\pi^+$ and $T_{cc}^+ \to D^0D^+\pi^0(\gamma)$ decays that uses the isospin symmetry for the $T_{cc}^+ \to D^*D$ transition[91] yields insights into the fundamental resonance properties, such as the pole position, the scattering length and the effective range. The observation of this $cc\bar{u}\bar{d}$ tetraquark candidate close to the $D^{*+}D^0$ threshold provides strong support for the theoretical approaches and models that predict the existence of a $bb\bar{u}\bar{d}$ tetraquark that is stable with respect to the strong and electromagnetic interactions.

Online content

Any methods, additional references, Nature Research reporting summaries, source data, extended data, supplementary information, acknowledgements, peer review information; details of author contributions and competing interests; and statements of data and code availability are available at https://doi.org/10.1038/s41567-022-01614-y.

Received: 7 September 2021; Accepted: 13 April 2022;
Published online: 16 June 2022

References

1. Gell-Mann, M. A schematic model of baryons and mesons. *Phys. Lett.* **8**, 214–215 (1964).
2. Zweig, G. *An SU$_3$Model for Strong Interaction Symmetry and Its Breaking, Version 1. Tech. Rep. CERN-TH-401* (CERN, 1964).
3. Zweig, G. *An SU$_3$ Model for Strong Interaction Symmetry and Its Breaking, Version 2. Tech. Rep. CERN-TH-412* (CERN, 1964).
4. Jaffe, R. L. Multiquark hadrons. I. Phenomenology of $Q^2\bar{Q}^2$ mesons. *Phys. Rev.* **D15**, 267–280 (1977).
5. Jaffe, R. L. Multi-quark hadrons. 2. Methods. *Phys. Rev.* **D15**, 281–289 (1977).
6. Rossi, G. C. & Veneziano, G. A possible description of baryon dynamics in dual and gauge theories. *Nucl. Phys.* **B123**, 507–545 (1977).
7. Jaffe, R. L. $Q^2\bar{Q}^2$ resonances in the baryon–antibaryon system. *Phys. Rev.* **D17**, 1444–1458 (1978).
8. Lipkin, H. J. New possibilities for exotic hadrons – anticharmed strange baryons. *Phys. Lett.* **B195**, 484–488 (1987).
9. Belle Collaboration, Choi, S. K., et al. Observation of a narrow charmoniumlike state in exclusive $B^{\pm}\to K^{\pm}\pi^+\pi^- J/\psi$ decays. *Phys. Rev. Lett.* **91**, 262001 (2003).
10. Belle Collaboration, Choi, S. K., et al. Observation of a resonancelike structure in the $\pi^{\pm}\psi'$ mass distribution in exclusive $B\to K\pi^{\pm}\psi'$ decays. *Phys. Rev. Lett.* **100**, 142001 (2008).
11. Belle Collaboration, Mizuk, R., et al. Observation of two resonance-like structures in the $\pi^+\chi_{c1}$ mass distribution in exclusive $\bar{B}^0 \to K^-\pi^+\chi_{c1}$ decays, *Phys. Rev.* **D78**, 072004 (2008).
12. CDF Collaboration, Aaltonen, T., et al. Evidence for a narrow near-threshold structure in the $J/\psi\phi$ mass spectrum in $B^+\to J/\psi\phi K^+$ decays. *Phys. Rev. Lett.* **102**, 242002 (2009).
13. Belle Collaboration, Bondar, A., et al. Observation of two charged bottomonium-like resonances in Υ(5S) decays. *Phys. Rev. Lett.* **108**, 122001 (2012).
14. BESIII Collaboration, Ablikim, M. et al. Observation of a charged charmoniumlike structure in $e^+e^-\to\pi^+\pi^- J/\psi$ at $\sqrt{s}=4.26$ GeV. *Phys. Rev. Lett.* **110**, 252001 (2013).
15. BESIII Collaboration, Ablikim, M., et al. Observation of a charged charmoniumlike structure $Z_c(4020)$ and search for the $Z_c(3900)$ in $e^+e^-\to\pi^+\pi^- h_c$. *Phys. Rev. Lett.* **111**, 242001 (2013).
16. BESIII Collaboration, Ablikim, M., et al. Observation of a charged charmoniumlike structure in $e^+e^- \to \left(D^*\bar{D}^*\right)^{\pm}\pi^{\mp}$ at $\sqrt{s}=4.26$ GeV. *Phys. Rev. Lett.* **112**, 132001 (2014).
17. D0 Collaboration, Abazov, V. M., et al. Search for the $X(4140)$ state in $B^+\to J/\psi\phi K^+$ decays with the D0 detector. *Phys. Rev.* **D89**, 012004 (2014).
18. CMS Collaboration, Chatrchyan, S. et al. Observation of a peaking structure in the $J/\psi\phi$ mass spectrum from $B^+\to J/\psi\phi K^+$ decays. *Phys. Lett.* **B734**, 261–281 (2014).
19. Belle Collaboration, Chilikin, K., et al. Experimental constraints on the spin and parity of the $Z(4430)^+$. *Phys. Rev.* **D88**, 074026 (2013).
20. Belle Collaboration, Liu, Z. Q., et al. Study of $e^+e^-\to\pi^+\pi^- J/\psi$ and observation of a charged charmoniumlike state at Belle. *Phys. Rev. Lett.* **110**, 252002 (2013). Erratum, ibid. **111**, 019901 (2013).
21. Belle Collaboration, Chilikin, K., et al. Observation of a new charged charmoniumlike state in $\bar{B}^0 \to J/\psi K^-\pi^+$ decays. *Phys. Rev.* **D90**, 112009 (2014).
22. LHCb Collaboration, Aaij, R., et al. Observation of the resonant character of the $Z(4430)^-$ state. *Phys. Rev. Lett.* **112**, 222002 (2014).
23. LHCb Collaboration, Aaij, R., et al. Observation of $J/\psi p$ resonances consistent with pentaquark states in $\Lambda_b^0 \to J/\psi p K^-$ decays. *Phys. Rev. Lett.* **115**, 072001 (2015).
24. LHCb Collaboration, Aaij, R., et al. Model-independent confirmation of the $Z(4430)^-$ state. *Phys. Rev.* **D92**, 112009 (2015).
25. LHCb Collaboration, Aaij, R., et al. Observation of exotic $J/\psi\phi$ structures from amplitude analysis of $B^+\to J/\psi\phi K^+$ decays. *Phys. Rev. Lett.* **118**, 022003 (2017).
26. LHCb Collaboration, Aaij, R., et al. Amplitude analysis of $B^+\to J/\psi\phi K^+$ decays. *Phys. Rev.* **D95**, 012002 (2017).
27. LHCb Collaboration, Aaij, R., et al. Evidence for a $\eta_c(1S)\pi^-$ resonance in $B^0\to\eta_c(1S)K^+\pi^-$ decays. *Eur. Phys. J.* **C78**, 1019 (2018).
28. LHCb Collaboration, Aaij, R., et al. Observation of a narrow pentaquark state, $P_c(4312)^+$, and of two-peak structure of the $P_c(4450)^+$. *Phys. Rev. Lett.* **122**, 222001 (2019).
29. LHCb Collaboration, Aaij, R., et al. Observation of structure in the J/ψ-pair mass spectrum. *Sci. Bull.* **65**, 1983–1993 (2020).
30. LHCb Collaboration, Aaij, R., et al. Model-independent study of structure in $B^+\to D^+D^-K^+$decays. *Phys. Rev. Lett.* **125**, 242001 (2020).
31. LHCb Collaboration, Aaij, R., et al. Amplitude analysis of the $B^+\to D^+D^-K^+$ decay. *Phys. Rev.* **D102**, 112003 (2020).
32. LHCb Collaboration, Aaij, R., et al. Study of $B_s^0 \to J/\psi\pi^+\pi^-K^+K^-$ decays. *J. High Energy Phys.* **02**, 024 (2021).
33. LHCb Collaboration, Aaij, R., et al. Evidence of a $J/\psi\Lambda$ structure and observation of excited Ξ^- states in the $\Xi_b^- \to J/\psi\Lambda K^-$ decay. *Sci. Bull.* **66**, 1278–1287 (2021).
34. LHCb Collaboration, Aaij, R., et al. Observation of new resonances decaying into $J/\psi K^+$ and $J/\psi\phi$. *Phys. Rev. Lett.* **127**, 082001 (2021).
35. BESIII Collaboration, Ablikim, M., et al. Observation of a near-threshold structure in the K^+ recoil-mass spectra in $e^+e^- \to K^+\left(D_s^-D^{*0}+D_s^{*-}D^0\right)$. *Phys. Rev. Lett.* **126**, 102001 (2021).
36. LHCb Collaboration, Aaij, R., et al. Evidence for a new structure in the $J/\psi p$ and $B_s^0 \to J/\psi p\bar{p}$ systems in $B_s^0 J/\psi p\bar{p}$ decays. *Phys. Rev. Lett.* **128**, 062001 (2022).
37. Brambilla, N., et al. The *XYZ* states: experimental and theoretical status and perspectives. *Phys. Rept.* **873**, 1–154 (2020).

38. Particle Data Group, Zyla, P. A., et al. Review of particle physics. *Prog. Theor. Exp. Phys.* **2020**, 083C01 (2020). Update: http://pdglive.lbl.gov/ (2021)
39. Oset, E. et al. Tetra and pentaquarks from the molecular perspective. *EPJ Web Conf.* **199**, 01003 (2019).
40. Richard, J.-M. Exotic hadrons: review and perspectives. *Few Body Syst.* **57**, 1185–1212 (2016).
41. Guo, F.-K. et al. Hadronic molecules. *Rev. Mod. Phys.* **90**, 015004 (2018).
42. Martinez Torres, A., Khemchandani, K. P., Roca, L. & Oset, E. Few-body systems consisting of mesons. *Few Body Syst.* **61**, 35 (2020).
43. Ali, A., Maiani, L. and Polosa, A. D. *Multiquark Hadrons* (Cambridge Univ. Press, 2019).
44. Ader, J. P., Richard, J.-M. & Taxil, P. Do narrow heavy multiquark states exist? *Phys. Rev.* **D25**, 2370–2382 (1982).
45. l. Ballot, J. & Richard, J. M. Four quark states in additive potentials. *Phys. Lett.* **B123**, 449–451 (1983).
46. Zouzou, S., Silvestre-Brac, B., Gignoux, C. & Richard, J. M. Four quark bound states. *Z. Phys.* **C30**, 457–468 (1986).
47. Lipkin, H. J. A model-independent approach to multiquark bound states. *Phys. Lett.* **B172**, 242–247 (1986).
48. Heller, L. & Tjon, J. A. On the existence of stable dimesons. *Phys. Rev.* **D35**, 969–974 (1987).
49. Manohar, A. V. & Wise, M. B. Exotic $QQ\bar{q}\bar{q}$ states in QCD. *Nucl. Phys.* **B399**, 17–33 (1993).
50. LHCb Collaboration, Aaij, R, et al. Observation of the doubly charmed baryon Ξ_{cc}^{++}. *Phys. Rev. Lett.* **119**, 112001 (2017).
51. LHCb Collaboration, Aaij, R., et al. First observation of the doubly charmed baryon decay $\Xi_{cc}^{++} \to \Xi_c^+ \pi^+$. *Phys. Rev. Lett.* **121**, 162002 (2018).
52. LHCb Collaboration, Aaij, R., et al. Precision measurement of the Ξ_{cc}^{++} mass. *J. High Energy Phys.* **02**, 049 (2020).
53. Karliner, M. & Rosner, J. L. Discovery of doubly-charmed Ξ_{cc} baryon implies a stable $bb\bar{u}\bar{d}$ tetraquark. *Phys. Rev. Lett.* **119**, 202001 (2017).
54. Carlson, J., Heller, L. & Tjon, J. A. Stability of dimesons. *Phys. Rev.* **D37**, 744–753 (1988).
55. Silvestre-Brac, B. & Semay, C. Systematics of $L = 0$ $q^2\bar{q}^2$ systems. *Z. Phys.* **C57**, 273–282 (1993).
56. Semay, C. & Silvestre-Brac, B. Diquonia and potential models. *Z. Phys.* **C61**, 271–275 (1994).
57. Moinester, M. A. How to search for doubly charmed baryons and tetraquarks. *Z. Phys.* **A355**, 349–362 (1996).
58. Pepin, S., Stancu, F., Genovese, M. & Richard, J.-M. Tetraquarks with color blind forces in chiral quark models. *Phys. Lett.* **B393**, 119–123 (1997).
59. Gelman, B. A. & Nussinov, S. Does a narrow tetraquark $cc\bar{u}\bar{d}$ state exist? *Phys. Lett.* **B551**, 296–304 (2003).
60. Vijande, J., Fernandez, F., Valcarce, A. & Silvestre-Brac, B. Tetraquarks in a chiral constituent quark model. *Eur. Phys. J.* **A19**, 383–389 (2004).
61. Janc, D. & Rosina, M. The $T_{cc} = DD'$ molecular state. *Few Body Syst.* **35**, 175–196 (2004).
62. Navarra, F. S., Nielsen, M. & Lee, S. H. QCD sum rules study of QQ $-$ $\bar{u}\bar{d}$ mesons. *Phys. Lett.* **B649**, 166–172 (2007).
63. Vijande, J., Weissman, E., Valcarce, A. & Barnea, N. Are there compact heavy four-quark bound states? *Phys. Rev.* **D76**, 094027 (2007).
64. Ebert, D., Faustov, R. N., Galkin, V. O. & Lucha, W. Masses of tetraquarks with two heavy quarks in the relativistic quark model. *Phys. Rev.* **D76**, 114015 (2007).
65. Lee, S. H. & Yasui, S. Stable multiquark states with heavy quarks in a diquark model. *Eur. Phys. J.* **C64**, 283–295 (2009).
66. Yang, Y., Deng, C., Ping, J. & Goldman, T. S-wave $QQ\bar{q}\bar{q}$ state in the constituent quark model. *Phys. Rev.* **D80**, 114023 (2009).
67. Li, N., Sun, Z.-F., Liu, X., Zhu, S.-L., Liu, X. & Zhu, S.-L. Coupled-channel analysis of the possible $D(*)D(*)$, $B(*)B(*)$ and $D(*)B(*)$ molecular states. *Phys. Rev. D.* **88**, 11408 (2013).
68. Feng, G.-Q., Guo, X.-H., and Zou B.-S. $QQ'\bar{u}\bar{d}$ bound state in the Bethe–Salpeter equation approach. (2013), Preprint at http://arxiv.org/abs/1309.7813
69. Luo, S.-Q. et al. Exotic tetraquark states with the $qq\bar{Q}\bar{Q}$ configuration. *Eur. Phys. J.* **C77**, 709 (2017).
70. Eichten, E. J. & Quigg, C. Heavy-quark symmetry implies stable heavy tetraquark mesons $Q_iQ_j\bar{q}_k\bar{q}_l$. *Phys. Rev. Lett.* **119**, 202002 (2017).
71. Wang, Z.-G. Analysis of the axialvector doubly heavy tetraquark states with QCD sum rules. *Acta Phys. Polon.* **B49**, 1781–1800 (2018).
72. Park, W., Noh, S. & Lee, S. H. Masses of the doubly heavy tetraquarks in a constituent quark model. *Acta Phys. Polon.* **B50**, 1151–1157 (2019).
73. Junnarkar, P., Mathur, N. & Padmanath, M. Study of doubly heavy tetraquarks in lattice QCD. *Phys. Rev.* **D99**, 034507 (2019).
74. Deng, C., Chen, H. & Ping, J. Systematical investigation on the stability of doubly heavy tetraquark states. *Eur. Phys. J.* **A56**, 9 (2020).
75. Liu, M.-Z. et al. Heavy-quark spin and flavor symmetry partners of the X(3872) revisited: what can we learn from the one boson exchange model? *Phys. Rev.* **D99**, 094018 (2019).
76. Maiani, L., Polosa, A. D. & Riquer, V. Hydrogen bond of QCD in doubly heavy baryons and tetraquarks. *Phys. Rev.* **D100**, 074002 (2019).
77. Yang, G., Ping, J. & Segovia, J. Doubly-heavy tetraquarks. *Phys. Rev.* **D101**, 014001 (2020).
78. Tan, Y., Lu, W. & Ping, J. $QQ\bar{q}\bar{q}$ in a chiral constituent quark model. *Eur. Phys. J. Plus* **135**, 716 (2020).
79. Lü, Q.-F., Chen, D.-Y. & Dong, Y.-B. Masses of doubly heavy tetraquarks $T_{QQ'}$ in a relativized quark model. *Phys. Rev.* **D102**, 034012 (2020).
80. Braaten, E., He, L.-P. & Mohapatra, A. Masses of doubly heavy tetraquarks with error bars. *Phys. Rev.* **D103**, 016001 (2021).
81. Gao, D., et al. Masses of doubly heavy tetraquark states with isospin $= \frac{1}{2}$ and 1 and spin-parity $1^{+\pm}$. (2020). Preprint at http://arxiv.org/abs/2007.15213
82. Cheng, J.-B. et al. Double-heavy tetraquark states with heavy diquark–antiquark symmetry. *Chin. Phys. C* **45**, 043102 (2021).
83. Noh, S., Park, W. & Lee, S. H. Doubly heavy tetraquarks, $qq'\bar{Q}\bar{Q}'$, in a nonrelativistic quark model with a complete set of harmonic oscillator bases. *Phys. Rev.* **D103**, 114009 (2021).
84. Faustov, R. N., Galkin, V. O. & Savchenko, E. M. Heavy tetraquarks in the relativistic quark model. *Universe* **7**, 94 (2021).
85. Ikeda, Y. et al. Charmed tetraquarks T_{cc} and T_{cs} from dynamical lattice QCD simulations. *Phys. Lett.* **B729**, 85–90 (2014).
86. Hadron Spectrum Collaboration, Cheung, G. K. C., et al. Tetraquark operators in lattice QCD and exotic flavour states in the charm sector. *J. High Energy Phys.* **11**, 033 (2017).
87. Francis, A., Hudspith, R. J., Lewis, R. & Maltman, K. Evidence for charm-bottom tetraquarks and the mass dependence of heavy–light tetraquark states from lattice QCD. *Phys. Rev.* **D99**, 054505 (2019).
88. LHCb Collaboration, Alves A. A., Jr., et al. The LHCb detector at the LHC. *J. Instrum.* **3** S08005 (2008).
89. LHCb Collaboration, Aaij, R., et al. LHCb detector performance. *Int. J. Mod. Phys.* **A30**, 1530022 (2015).
90. LHCb Collaboration, Aaij, R., et al. Observation of double charm production involving open charm in pp collisions at $\sqrt{s} = 7$ TeV. *J. High Energy Phys.* **06**, 141 (2012). Addendum ibid. **03**, 108 (2014).
91. LHCb Collaboration, Aaij, R., et al. Study of a doubly charmed tetraquark state. *Nat. Commun.* https://doi.org/10.1038/s41567-022-01614-y (2022).
92. LHCb Collaboration, Aaij, R., et al. Study of the line shape of the $\chi_{c1}(3872)$ state. *Phys. Rev.* **D102**, 092005 (2020).
93. LHCb Collaboration, Aaij, R., et al. Study of the $\psi_2(3823)$ and $\chi_{c1}(3872)$ states in $B^+ \to \left(J/\psi\pi^+\pi^-\right) K^+$ decays. *J. High Energy Phys.* **08**, 123 (2020).
94. LHCb Collaboration, Aaij, R., et al. Precision measurement of D meson mass differences. *J. High Energy Phys.* **06**, 065 (2013).

Methods

Experimental setup. The LHCb detector[88,89] is a single-arm forward spectrometer covering the pseudorapidity range of $2<\eta<5$, designed to study particles containing b or c quarks. The detector includes a high-precision tracking system consisting of a silicon-strip vertex detector surrounding the pp interaction region, a large-area silicon-strip detector located upstream of a dipole magnet with a bending power of about 4 T m and three stations of silicon-strip detectors and straw drift tubes placed downstream of the magnet. The tracking system provides a measurement of the momentum, p, of charged particles with a relative uncertainty that varies from 0.5% at low momentum to 1.0% at 200 GeV c^{-1}. The minimum distance of a track to a primary pp collision vertex, the impact parameter, is measured with a resolution of $(15+29/p_{\rm T})\,\mu$m, where $p_{\rm T}$ is the component of the momentum transverse to the beam, in GeV c^{-1}. Different types of charged hadrons are distinguished using information from two ring-imaging Cherenkov detectors[95]. Photons, electrons and hadrons are identified by a calorimeter system consisting of scintillating-pad and preshower detectors and an electromagnetic and a hadronic calorimeter. Muons are identified by a system composed of alternating layers of iron and multiwire proportional chambers. The online event selection is performed by a trigger consisting of a hardware stage, based on information from the calorimeter and muon systems, followed by a software stage, which applies full event reconstruction. The trigger selection algorithms are primarily based on identifying key characteristics of beauty and charm hadrons and their decay products, such as high-$p_{\rm T}$ final state particles, and a decay vertex that is significantly displaced from any of the pp interaction vertices in the event.

Simulated samples. Simulation is required to model the effects of the detector acceptance and resolution and the imposed selection requirements. In the simulation, pp collisions are generated using PYTHIA with a specific LHCb configuration[96]. Decays of unstable particles are described by EVTGEN[97]. The interaction of the generated particles with the detector, and its response, are implemented using the GEANT4 toolkit as described in ref. [98].

Selection. The selection of $D\to K^-\pi^+$ candidates and $D^0D^0\pi^+$ combinations is similar to those used in ref. [90]. Kaon and pion candidates are selected from well-reconstructed tracks within the acceptance of the spectrometer. Particle identification is provided using information from the ring-imaging Cherenkov detectors. Kaons and pions that have transverse momenta larger than 250 MeV c^{-1} and are inconsistent with being produced in a pp interaction vertex are combined together to form D^0 candidates. The resulting D^0 candidates are required to have good vertex quality, mass within ±65 MeV of the known D^0 mass[38] (the mass resolution for the $D\to K^-\pi^+$ signal being 7 MeV), transverse momentum larger than 1 GeV c^{-1}, decay time longer than 100 μm c^{-1} and a momentum direction that is consistent with the vector from the primary to the secondary vertex. Selected pairs of D^0 candidates consistent with originating from a common primary vertex are then combined with pion candidates of the same charge as the pions from the $D\to K^-\pi^+$ decay candidates to form $D^0D^0\pi^+$ candidates. At least one of the two $D^0\pi^+$ combinations is required to have good vertex quality and mass not exceeding the known D^0 mass by more than 155 MeV. For each $D^0D^0\pi^+$ candidate, a kinematic fit[99] is performed. This fit requires both D^0 candidates and a pion to originate from the same primary vertex. A requirement on the quality of this fit is applied to further suppress combinatorial background and reduce the background from D^0 candidates produced in two independent pp interactions or in decays of beauty hadrons[90]. To suppress the background from kaon and pion candidates reconstructed from one common track, all track pairs of the same charge are required to have an opening angle inconsistent with being zero and the mass of the combination inconsistent with the sum of the masses of the two constituents.

Non-D^0 background subtraction. The two-dimensional distribution of the mass of one D^0 candidate versus the mass of the other D^0 candidate from selected $D^0D^0\pi^+$ combinations is used to subtract the background due to fake D^0 candidates. The procedure employs the sPlot technique[100], where an extended, unbinned, maximum-likelihood fit to the two-dimensional distribution is performed. The signal is described using a modified Novosibirsk function, and the background is modelled by a product of an exponential function and a positive polynomial function[90]. Each candidate is assigned a positive weight for being signal-like or a negative weight for being background-like, with the masses of the two D^0 candidates as the discriminating variables. All candidates are then retained, and the weights are used in the further analysis for the statistical subtraction of the non-D^0 background.

Contributions from the $D^0\overline{D}^0$ oscillations. A hypothetical, narrow, charmonium-like state decaying into the $D^0\overline{D}^0\pi^+$ final state, followed by the $\overline{D}^0\to D^0$ transition or doubly Cabibbo-suppressed decay $\bar{D}^0\to K^-\pi^+$, would produce a narrow signal in the reconstructed $D^0D^0\pi^+$ mass spectrum. If the observed, narrow, near-threshold peak in the reconstructed $D^0D^0\pi^+$ system is caused by the $D^0\overline{D}^0$ oscillations or doubly Cabibbo-suppressed decays, a much larger signal should be visible in the reconstructed $D^0\overline{D}^0\pi^+$ mass spectrum at the same mass. No such structure is observed (see fig. 9 in ref. [91]).

Systematic uncertainties. Several sources of systematic uncertainty on the mass $\delta m_{\rm BW}$ and width $\Gamma_{\rm BW}$ of the T_{cc}^+ state have been evaluated. The largest systematic uncertainty is related to the fit model and is studied using a set of alternative parameterizations and pseudoexperiments. For each alternative model, an ensemble of pseudoexperiments is produced. Each is generated using the model under consideration with parameters obtained from a fit to the data. A subsequent fit with the default model to each pseudoexperiment is performed and the mean values of the parameters of interest over the ensemble are evaluated. The absolute value of the difference between the ensemble mean and the value of the parameter obtained from the fit to the data sample is used to characterize the difference between the alternative model and the default model. The maximal value of such a difference over the considered set of alternative models is taken as the corresponding systematic uncertainty for the mass $\delta m_{\rm BW}$ and width $\Gamma_{\rm BW}$ of the T_{cc}^+ state. The following sources of systematic uncertainties related to the fit model are considered:

- The imperfect knowledge of the detector resolution model: To estimate the associated systematic uncertainty, alternative resolution functions are studied, namely a symmetric variant of an Apollonios function, a modified Gaussian function with symmetric power-law tails on both sides of the distribution, a generalized symmetric Student's t-distribution, a symmetric Johnson's $S_{\rm U}$ distribution and a modified Novosibirsk function.
- The difference in the detector resolution due to imperfect modelling: A correction factor of 1.05 for the resolution is applied for the default fit to account for such a difference. This factor was studied for several other decays measured with the LHCb detector and found to lie between 1.0 and 1.1 (refs. [92,93]). For decays with relatively low-momentum tracks, this factor is close to 1.05. The factor is also cross-checked using large samples of $D^{*+}\to D^0\pi^+$ decays, where a value of 1.06 is obtained. To assess the systematic uncertainty related to this factor, detector resolution models with correction factors of 1.0 and 1.1 are studied as alternative models.
- The parameterization of the background component: To assess the associated systematic uncertainty, the order of the positive polynomial function used for the baseline fit is varied. In addition, to estimate the possible effect of a small contribution from $D^0D^0\pi^+$ combinations without an intermediate D^{*+} meson, a three-body background component is added to the fit. This component is described by a product of the three-body phase-space function and a positive linear or second-order polynomial function. The contribution from the non-resonant $D^0D^0\pi^+$ background is negligible in the low-mass region due to the $O(Q^2)$ scaling of the three-body phase-space factor near threshold.
- The model parameters of the BW function: Alternative parameterizations include different choices for the decay structure, $m_A=m_{D^0}$ and $m_B=m_{D^0}+m_{\pi^+}$; the meson radius, 1.5 GeV^{-1} and 5 GeV^{-1}, and the orbital angular momentum between A and B particles, corresponding to S- and D-waves. The effect of the different decay structure and the choice of the meson radius is smaller than 1 keV c^{-2} and 1 keV for the $\delta m_{\rm BW}$ and $\Gamma_{\rm BW}$ parameters, respectively. The parameters of interest are more sensitive to the choice of orbital angular momentum, in which the S-wave function gives larger $\delta m_{\rm BW}$ and smaller $\Gamma_{\rm BW}$, whereas the D-wave function corresponds to smaller $\delta m_{\rm BW}$ and larger $\Gamma_{\rm BW}$. As the S-wave and D-wave imply that the quantum numbers of the T_{cc}^+ state differ from $J^{\rm P}=1^+$, the corresponding systematic uncertainty is considered separately and is not included it in the total systematic uncertainty.

The calibration of the momentum scale of the tracking system is based upon large calibration samples of $B^+\to J/\psi K^+$ and $J/\psi\to\mu^+\mu^-$ decays. The accuracy of this procedure has been checked using other fully reconstructed B decays together with two-body $\Upsilon(nS)$ and K_S^0 decays, and the largest deviation of the bias in the momentum scale of $\delta\alpha=3\times10^{-4}$ is taken as the uncertainty[94]. This is then propagated to uncertainties for the parameters of interest using simulated samples, where momentum scale corrections of $(1\pm\delta\alpha)$ are applied. Half of the difference between the peak locations obtained with the $1+\delta\alpha$ and $1-\delta\alpha$ corrections applied to the same simulated sample is taken as an estimate of the systematic uncertainty due to the momentum scale. The main contribution to this uncertainty is due to the bachelor pion track, since the D^0 mass constraint reduces the contributions from the kaon and pion tracks originating from D^0 meson decays.

In the reconstruction, the momenta of the charged tracks are corrected for the energy loss in the detector material. The energy loss corrections are calculated using the Bethe–Bloch formula. The amount of material traversed in the tracking system by a charged particle is known to 10% accuracy. To assess the corresponding uncertainty, the magnitude of the calculated corrections is varied by ±10%. Half of the difference between the peak locations obtained with the +10% and −10% corrections applied to the same simulated sample is taken as an estimate of the systematic uncertainty due to the energy loss corrections.

The mass of the $D^0D^0\pi^+$ combinations is calculated with both D^0 candidate masses constrained to the known D^0 meson mass[38]. This procedure removes the uncertainty on the $\delta m_{\rm BW}$ parameter related to imprecise knowledge of the D^0 mass. In contrast, the small uncertainty of 2 keV c^{-2} for the known $D^{*+}-D^0$ mass difference[38] directly affects the $\delta m_{\rm BW}$ value and is therefore assigned as the corresponding systematic uncertainty.

Data availability

LHCb data used in this analysis will be released according to the LHCb external data access policy, that can be downloaded from http://opendata.cern.ch/record/410/files/LHCb-Data-Policy.pdf.

The raw data shown in all of the figures of this manuscript can be downloaded from https://cds.cern.ch/record/2780001, where no access codes are required. In addition, the unbinned background-subtracted data, shown in Fig. 1 have been added to the HEPData record at https://www.hepdata.net/record/ins1915457.

Code availability

LHCb software used to process the data analysed in this manuscript is available at GitLab repository https://gitlab.cern.ch/lhcb. The specific software used in data analysis is available at Zenodo repository https://doi.org/10.5281/zenodo.5595937.

References

95. Adinolfi, M. et al. Performance of the LHCb RICH detector at the LHC. *Eur. Phys. J.* **C73**, 2431 (2013).
96. Belyaev, I. et al. Handling of the generation of primary events in Gauss, the LHCb simulation framework. *J. Phys. Conf. Ser.* **331**, 032047 (2011).
97. Lange, D. J. The EvtGen particle decay simulation package. *Nucl. Instrum. Meth.* **A462**, 152–155 (2001).
98. Clemencic, M. et al. The LHCb simulation application, Gauss: design, evolution and experience. *J. Phys. Conf. Ser.* **331**, 032023 (2011).
99. Hulsbergen, W. D. Decay chain fitting with a Kalman filter. *Nucl. Instrum. Methods* **A552**, 566–575 (2005).
100. Pivk, M. & Le Diberder, F. R. sPlot: a statistical tool to unfold data distributions. *Nucl. Instrum. Methods* **A555**, 356–369 (2005).

Acknowledgements

This Letter is dedicated to the memory of our dear colleague Simon Eidelman, whose friendship, deep physics insights and contributions to improving the quality of our papers were greatly appreciated and will be missed. We express our gratitude to our colleagues in the CERN accelerator departments for the excellent performance of the LHC. We thank the technical and administrative staff at the LHCb institutes. We acknowledge support from CERN and from the following national agencies: CAPES, CNPq, FAPERJ and FINEP (Brazil); MOST and NSFC (China); CNRS/IN2P3 (France); BMBF, DFG and MPG (Germany); INFN (Italy); NWO (the Netherlands); MNiSW and NCN (Poland); MEN/IFA (Romania); MSHE (Russia); MICINN (Spain); SNSF and SER (Switzerland); NASU (Ukraine); STFC (United Kindgom); DOE NP and NSF (United States). We acknowledge the computing resources that are provided by CERN, IN2P3 (France), KIT and DESY (Germany), INFN (Italy), SURF (the Netherlands), PIC (Spain), GridPP (United Kingdom), RRCKI and Yandex LLC (Russia), CSCS (Switzerland), IFIN-HH (Romania), CBPF (Brazil), PL-GRID (Poland) and NERSC (United States). We are indebted to the communities behind the multiple open-source software packages on which we depend. Individual groups or members have received support from ARC and ARDC (Australia); AvH Foundation (Germany); EPLANET, Marie Skłodowska-Curie Actions and ERC (European Union); A*MIDEX, ANR, IPhU and Labex P2IO, and Région Auvergne-Rhône-Alpes (France); Key Research Program of Frontier Sciences of CAS, CAS PIFI, CAS CCEPP, Fundamental Research Funds for the Central Universities, and Sci. & Tech. Program of Guangzhou (China); RFBR, RSF and Yandex LLC (Russia); GVA, XuntaGal and GENCAT (Spain); the Leverhulme Trust, the Royal Society and UKRI (United Kingdom).

Author contributions

All contributing authors, as listed at the end of this manuscript, have contributed to the publication, being variously involved in the design and construction of the detector, in writing software, calibrating sub-systems, operating the detector and acquiring data and finally analysing the processed data.

Competing interests

The authors declare no competing interests.

Additional information

Supplementary information The online version contains supplementary material available at https://doi.org/10.1038/s41567-022-01614-y.

Correspondence and requests for materials should be addressed to I. Belyaev.

Peer review information *Nature Physics* thanks Iain Bertram, Nora Brambilla, and Zhiqing Liu for their contribution to the peer review of this work. This article has been peer reviewed as part of Springer Nature's Guided Open Access initiative.

Reprints and permissions information is available at www.nature.com/reprints.

LHCb Collaboration

R. Aaij[1], A. S. W. Abdelmotteleb[2], C. Abellán Beteta[3], F. J. Abudinen Gallego[2], T. Ackernley[4], B. Adeva[5], M. Adinolfi[6], H. Afsharnia[7], C. Agapopoulou[8], C. A. Aidala[9], S. Aiola[10], Z. Ajaltouni[7], S. Akar[11], J. Albrecht[12], F. Alessio[13], M. Alexander[14], A. Alfonso Albero[15], Z. Aliouche[16], G. Alkhazov[17], P. Alvarez Cartelle[18], S. Amato[19], J. L. Amey[6], Y. Amhis[20], L. An[13], L. Anderlini[21], A. Andreianov[17], M. Andreotti[22], F. Archilli[23], A. Artamonov[24], M. Artuso[25], K. Arzymatov[26], E. Aslanides[27], M. Atzeni[3], B. Audurier[28], S. Bachmann[23], M. Bachmayer[29], J. J. Back[2], P. Baladron Rodriguez[5], V. Balagura[28], W. Baldini[22], J. Baptista Leite[30], M. Barbetti[21,88], R. J. Barlow[16], S. Barsuk[20], W. Barter[31], M. Bartolini[32,89], F. Baryshnikov[33], J. M. Basels[34], S. Bashir[35], G. Bassi[36], B. Batsukh[25], A. Battig[12], A. Bay[29], A. Beck[2], M. Becker[12], F. Bedeschi[36], I. Bediaga[30], A. Beiter[25], V. Belavin[26], S. Belin[37], V. Bellee[3], K. Belous[24], I. Belov[38], I. Belyaev[39] ✉, G. Bencivenni[40], E. Ben-Haim[8], A. Berezhnoy[38], R. Bernet[3], D. Berninghoff[23], H. C. Bernstein[25], C. Bertella[13], A. Bertolin[41], C. Betancourt[3], F. Betti[13], Ia. Bezshyiko[3], S. Bhasin[6], J. Bhom[42], L. Bian[43], M. S. Bieker[12], S. Bifani[44], P. Billoir[8], M. Birch[31], F. C. R. Bishop[18], A. Bitadze[16], A. Bizzeti[21,90], M. Bjørn[45], M. P. Blago[13], T. Blake[2], F. Blanc[29], S. Blusk[25], D. Bobulska[14], J. A. Boelhauve[12], O. Boente Garcia[5], T. Boettcher[11], A. Boldyrev[46], A. Bondar[47], N. Bondar[17,13], S. Borghi[16], M. Borisyak[26], M. Borsato[23], J. T. Borsuk[42], S. A. Bouchiba[29], T. J. V. Bowcock[4], A. Boyer[13], C. Bozzi[22], M. J. Bradley[31], S. Braun[48], A. Brea Rodriguez[5], J. Brodzicka[42], A. Brossa Gonzalo[2], D. Brundu[37], A. Buonaura[3], L. Buonincontri[41], A. T. Burke[16], C. Burr[13], A. Bursche[49], A. Butkevich[50], J. S. Butter[1], J. Buytaert[13], W. Byczynski[13], S. Cadeddu[37], H. Cai[43], R. Calabrese[22,91], L. Calefice[12,8], L. Calero Diaz[40], S. Cali[40], R. Calladine[44], M. Calvi[51,92], M. Calvo Gomez[52], P. Camargo Magalhaes[6], P. Campana[40], A. F. Compoverde Quezada[53], S. Capelli[51,92], L. Capriotti[54,93], A. Carbone[54,93], G. Carboni[55], R. Cardinale[32,89], A. Cardini[37], I. Carli[56], P. Carniti[51,92], L. Carus[34], K. Carvalho Akiba[1], A. Casais Vidal[5], G. Casse[4], M. Cattaneo[13], G. Cavallero[13], S. Celani[29], J. Cerasoli[27], D. Cervenkov[45], A. J. Chadwick[4], M. G. Chapman[6], M. Charles[8], Ph. Charpentier[13], G. Chatzikonstantinidis[44], C. A. Chavez Barajas[4], M. Chefdeville[57], C. Chen[58], S. Chen[56], A. Chernov[42], V. Chobanova[5], S. Cholak[29], M. Chrzaszcz[42], A. Chubykin[17], V. Chulikov[17], P. Ciambrone[40], M. F. Cicala[2], X. Cid Vidal[5], G. Ciezarek[13], P. E. L. Clarke[59], M. Clemencic[13], H. V. Cliff[18], J. Closier[13], J. L. Cobbledick[16], V. Coco[13], J. A. B. Coelho[20], J. Cogan[27], E. Cogneras[7], L. Cojocariu[60], P. Collins[13], T. Colombo[13], L. Congedo[61,94], A. Contu[37], N. Cooke[44], G. Coombs[14], I. Corredoira[5], G. Corti[13], C. M. Costa Sobral[2], B. Couturier[13], D. C. Craik[62], J. Crkovská[63], M. Cruz Torres[30], R. Currie[59], C. L. Da Silva[63], S. Dadabaev[33], L. Dai[64], E. Dall'Occo[12], J. Dalseno[5], C. D'Ambrosio[13], A. Danilina[39], P. d'Argent[13], J. E. Davies[16], A. Davis[16], O. De Aguiar Francisco[16], K. De Bruyn[65], S. De Capua[16], M. De Cian[29], J. M. De Miranda[30], L. De Paula[19], M. De Serio[61,94], D. De Simone[3], P. De Simone[40], F. De Vellis[12], J. A. de Vries[66], C. T. Dean[63], F. Debernardis[61,94], D. Decamp[57], V. Dedu[27], L. Del Buono[8], B. Delaney[18], H.-P. Dembinski[12], A. Dendek[35], V. Denysenko[3], D. Derkach[46], O. Deschamps[7], F. Desse[20], F. Dettori[37,95], B. Dey[67], A. Di Cicco[40], P. Di Nezza[40], S. Didenko[33], L. Dieste Maronas[5], H. Dijkstra[13], V. Dobishuk[68], C. Dong[58], A. M. Donohoe[69], F. Dordei[37], A. C. dos Reis[30], L. Douglas[14], A. Dovbnya[70], A. G. Downes[57], M. W. Dudek[42], L. Dufour[13], V. Duk[71], P. Durante[13], J. M. Durham[63], D. Dutta[16], A. Dziurda[42], A. Dzyuba[17], S. Easo[72], U. Egede[73], V. Egorychev[39], S. Eidelman[47,96,109], S. Eisenhardt[59], S. Ek-In[29], L. Eklund[14,74], S. Ely[25], A. Ene[60], E. Epple[63], S. Escher[34], J. Eschle[3], S. Esen[8], T. Evans[13], A. Falabella[54], J. Fan[58], Y. Fan[53], B. Fang[43], S. Farry[4], D. Fazzini[51,92], M. Féo[13], A. Fernandez Prieto[5], A. D. Fernez[48], F. Ferrari[54,93], L. Ferreira Lopes[29], F. Ferreira Rodrigues[19], S. Ferreres Sole[1], M. Ferrillo[3], M. Ferro-Luzzi[13], S. Filippov[50], R. A. Fini[61],

M. Fiorini[22,91], M. Firlej[35], K. M. Fischer[45], D. S. Fitzgerald[9], C. Fitzpatrick[16], T. Fiutowski[35], A. Fkiaras[13], F. Fleuret[28], M. Fontana[8], F. Fontanelli[32,89], R. Forty[13], D. Foulds-Holt[18], V. Franco Lima[4], M. Franco Sevilla[48], M. Frank[13], E. Franzoso[22], G. Frau[23], C. Frei[13], D. A. Friday[14], J. Fu[53], Q. Fuehring[12], E. Gabriel[1], G. Galati[61,94], A. Gallas Torreira[5], D. Galli[54,93], S. Gambetta[59,13], Y. Gan[58], M. Gandelman[19], P. Gandini[10], Y. Gao[75], M. Garau[37], L. M. Garcia Martin[2], P. Garcia Moreno[15], J. García Pardiñas[51,92], B. Garcia Plana[5], F. A. Garcia Rosales[28], L. Garrido[15], C. Gaspar[13], R. E. Geertsema[1], D. Gerick[23], L. L. Gerken[12], E. Gersabeck[16], M. Gersabeck[16], T. Gershon[2], D. Gerstel[27], L. Giambastiani[41], V. Gibson[18], H. K. Giemza[76], A. L. Gilman[45], M. Giovannetti[40,97], A. Gioventù[5], P. Gironella Gironell[15], L. Giubega[60], C. Giugliano[13,22,91], K. Gizdov[59], E. L. Gkougkousis[13], V. V. Gligorov[8], C. Göbel[77], E. Golobardes[52], D. Golubkov[39], A. Golutvin[31,33], A. Gomes[30,98], S. Gomez Fernandez[15], F. Goncalves Abrantes[45], M. Goncerz[42], G. Gong[58], P. Gorbounov[39], I. V. Gorelov[38], C. Gotti[51], E. Govorkova[13], J. P. Grabowski[23], T. Grammatico[8], L. A. Granado Cardoso[13], E. Graugés[15], E. Graverini[29], G. Graziani[21], A. Grecu[60], L. M. Greeven[1], N. A. Grieser[56], L. Grillo[16], S. Gromov[33], B. R. Gruberg Cazon[45], C. Gu[58], M. Guarise[22], M. Guittiere[20], P. A. Günther[23], E. Gushchin[50], A. Guth[34], Y. Guz[24], T. Gys[13], T. Hadavizadeh[73], G. Haefeli[29], C. Haen[13], J. Haimberger[13], T. Halewood-leagas[4], P. M. Hamilton[48], J. P. Hammerich[4], Q. Han[78], X. Han[23], T. H. Hancock[45], E. B. Hansen[16], S. Hansmann-Menzemer[23], N. Harnew[45], T. Harrison[4], C. Hasse[13], M. Hatch[13], J. He[53,99], M. Hecker[31], K. Heijhoff[1], K. Heinicke[12], A. M. Hennequin[13], K. Hennessy[4], L. Henry[13], J. Heuel[34], A. Hicheur[19], D. Hill[29], M. Hilton[16], S. E. Hollitt[12], R. Hou[78], Y. Hou[57], J. Hu[23], J. Hu[49], W. Hu[78], X. Hu[58], W. Huang[53], X. Huang[43], W. Hulsbergen[1], R. J. Hunter[2], M. Hushchyn[46], D. Hutchcroft[4], D. Hynds[1], P. Ibis[12], M. Idzik[35], D. Ilin[17], P. Ilten[11], A. Inglessi[17], A. Ishteev[33], K. Ivshin[17], R. Jacobsson[13], H. Jage[34], S. Jakobsen[13], E. Jans[1], B. K. Jashal[79], A. Jawahery[48], V. Jevtic[12], F. Jiang[58], M. John[45], D. Johnson[13], C. R. Jones[18], T. P. Jones[2], B. Jost[13], N. Jurik[13], S. H. Kalavan Kadavath[35], S. Kandybei[70], Y. Kang[58], M. Karacson[13], M. Karpov[46], F. Keizer[13], D. M. Keller[25], M. Kenzie[2], T. Ketel[80], B. Khanji[12], A. Kharisova[81], S. Kholodenko[24], T. Kirn[34], V. S. Kirsebom[29], O. Kitouni[62], S. Klaver[1], N. Kleijne[36], K. Klimaszewski[76], M. R. Kmiec[76], S. Koliiev[68], A. Kondybayeva[33], A. Konoplyannikov[39], P. Kopciewicz[35], R. Kopecna[23], P. Koppenburg[1], M. Korolev[38], I. Kostiuk[1,68], O. Kot[68], S. Kotriakhova[22,17], P. Kravchenko[17], L. Kravchuk[50], R. D. Krawczyk[13], M. Kreps[2], F. Kress[31], S. Kretzschmar[34], P. Krokovny[47,96], W. Krupa[35], W. Krzemien[76], M. Kucharczyk[42], V. Kudryavtsev[47,96], H. S. Kuindersma[1,80], G. J. Kunde[63], T. Kvaratskheliya[39], D. Lacarrere[13], G. Lafferty[16], A. Lai[37], A. Lampis[37], D. Lancierini[3], J. J. Lane[16], R. Lane[6], G. Lanfranchi[40], C. Langenbruch[34], J. Langer[12], O. Lantwin[33], T. Latham[2], F. Lazzari[36,100], R. Le Gac[27], S. H. Lee[9], R. Lefèvre[7], A. Leflat[38], S. Legotin[33], O. Leroy[27], T. Lesiak[42], B. Leverington[23], H. Li[49], P. Li[23], S. Li[78], Y. Li[56], Y. Li[56], Z. Li[25], X. Liang[25], T. Lin[31], R. Lindner[13], V. Lisovskyi[12], R. Litvinov[37], G. Liu[49], H. Liu[53], Q. Liu[53], S. Liu[56], A. Lobo Salvia[15], A. Loi[37], J. Lomba Castro[5], I. Longstaff[14], J. H. Lopes[19], S. Lopez Solino[5], G. H. Lovell[18], Y. Lu[56], C. Lucarelli[21,88], D. Lucchesi[41,101], S. Luchuk[50], M. Lucio Martinez[1], V. Lukashenko[1,68], Y. Luo[58], A. Lupato[16], E. Luppi[22,91], O. Lupton[2], A. Lusiani[36,102], X. Lyu[53], L. Ma[56], R. Ma[53], S. Maccolini[54,93], F. Machefert[20], F. Maciuc[60], V. Macko[29], P. Mackowiak[12], S. Maddrell-Mander[6], O. Madejczyk[35], L. R. Madhan Mohan[6], O. Maev[17], A. Maevskiy[46], D. Maisuzenko[17], M. W. Majewski[35], J. J. Malczewski[42], S. Malde[45], B. Malecki[13], A. Malinin[82], T. Maltsev[47,96], H. Malygina[23], G. Manca[37,95], G. Mancinelli[27], D. Manuzzi[54,93], D. Marangotto[10,103], J. Maratas[7,104], J. F. Marchand[57], U. Marconi[54], S. Mariani[21,88], C. Marin Benito[13], M. Marinangeli[29], J. Marks[23], A. M. Marshall[6], P. J. Marshall[4], G. Martelli[71], G. Martellotti[83], L. Martinazzoli[13,92], M. Martinelli[51,92], D. Martinez Santos[5], F. Martinz Vidal[79], A. Massafferri[30], M. Materok[34], R. Matev[13], A. Mathad[3], V. Matiunin[39], C. Matteuzzi[51], K. R. Mattioli[9], A. Mauri[1],

E. Maurice[28], J. Mauricio[15], M. Mazurek[13], M. McCann[31], L. Mcconnell[69], T. H. Mcgrath[16], N. T. Mchugh[14], A. McNab[16], R. McNulty[69], J. V. Mead[4], B. Meadows[11], G. Meier[12], N. Meinert[84], D. Melnychuk[76], S. Meloni[51,92], M. Merk[1,66], A. Merli[10], L. Meyer Garcia[19], M. Mikhasenko[13], D. A. Milanes[85], E. Millard[2], M. Milovanovic[13], M. -N. Minard[57], A. Minotti[51,92], L. Minzoni[22,91], S. E. Mitchell[59], B. Mitreska[16], D. S. Mitzel[12], A. Mödden[12], R. A. Mohammed[45], R. D. Moise[31], S. Mokhnenko[46], T. Mombächer[5], I. A. Monroy[85], S. Monteil[7], M. Morandin[41], G. Morello[40], M. J. Morello[36,102], J. Moron[35], A. B. Morris[86], A. G. Morris[2], R. Mountain[25], H. Mu[58], F. Muheim[59,13], M. Mulder[13], D. Müller[13], K. Müller[3], C. H. Murphy[45], D. Murray[16], P. Muzzetto[37,13], P. Naik[6], T. Nakada[29], R. Nandakumar[72], T. Nanut[29], I. Nasteva[19], M. Needham[59], I. Neri[22], N. Neri[10,103], S. Neubert[86], N. Neufeld[13], R. Newcombe[31], E. M. Niel[20], S. Nieswand[34], N. Nikitin[38], N. S. Nolte[62], C. Normand[57], C. Nunez[9], A. Oblakowska-Mucha[35], V. Obraztsov[24], T. Oeser[34], D. P. O'Hanlon[6], S. Okamura[22], R. Oldeman[37,95], F. Oliva[59], M. E. Olivares[25], C. J. G. Onderwater[65], R. H. O'neil[59], J. M. Otalora Goicochea[19], T. Ovsiannikova[39], P. Owen[3], A. Oyanguren[79], K. O. Padeken[86], B. Pagare[2], P. R. Pais[13], T. Pajero[45], A. Palano[61], M. Palutan[40], Y. Pan[16], G. Panshin[81], A. Papanestis[72], M. Pappagallo[61,94], L. L. Pappalardo[22,91], C. Pappenheimer[11], W. Parker[48], C. Parkes[16], B. Passalacqua[22], G. Passaleva[21], A. Pastore[61], M. Patel[31], C. Patrignani[54,93], C. J. Pawley[66], A. Pearce[13], A. Pellegrino[1], M. Pepe Altarelli[13], S. Perazzini[54], D. Pereima[39], A. Periero Castro[5], P. Perret[7], M. Petric[14,13], K. Petridis[6], A. Petrolini[32,89], A. Petrov[82], S. Petrucci[59], M. Petruzzo[10], T. T. H. Pham[25], L. Pica[36,102], M. Piccini[71], B. Pietrzyk[57], G. Pietrzyk[29], M. Pili[45], D. Pinci[83], F. Pisani[13], M. Pizzichemi[51,13,92], P. K. Resmi[10], V. Placinta[60], J. Plews[44], M. Plo Casasus[5], F. Polci[8], M. Poli Lener[40], M. Poliakova[25], A. Poluektov[27], N. Polukhina[33,105], I. Polyakov[25], E. Polycarpo[19], S. Ponce[13], D. Popov[53,13], S. Popov[26], S. Poslavskii[24], K. Prasanth[42], L. Promberger[13], C. Prouve[5], V. Pugatch[68], V. Puill[20], H. Pullen[45], G. Punzi[36,106], H. Qi[58], W. Qian[53], J. Qin[53], N. Qin[58], R. Quagliani[29], B. Quintana[57], N. V. Raab[69], R. I. Rabadan Trejo[53], B. Rachwal[35], J. H. Rademacker[6], M. Rama[36], M. Ramos Pernas[2], M. S. Rangel[19], F. Ratnikov[26,46], G. Raven[80], M. Reboud[57], F. Redi[29], F. Reiss[16], C. Remon Alepuz[79], Z. Ren[58], V. Renaudin[45], R. Ribatti[36], S. Ricciardi[72], K. Rinnert[4], P. Robbe[20], G. Robertson[59], A. B. Rodrigues[29], E. Rodrigues[4], J. A. Rodriguez Lopez[85], E. R. R. Rodriguez Rodriguez[5], A. Rollings[45], P. Roloff[13], V. Romanovskiy[24], M. Romero Lamas[5], A. Romero Vidal[5], J. D. Roth[9], M. Rotondo[40], M. S. Rudolph[25], T. Ruf[13], R. A. Ruiz Fernandez[5], J. Ruiz Vidal[79], A. Ryzhikov[46], J. Ryzka[35], J. J. Saborido Silva[5], N. Sagidova[17], N. Sahoo[2], B. Saitta[37,95], M. Salomoni[13], C. Sanchez Gras[1], R. Santacesaria[83], C. Santamarina Rios[5], M. Santimaria[40], E. Santovetti[55,97], D. Saranin[33], G. Sarpis[34], M. Sarpis[86], A. Sarti[83], C. Satriano[83,107], A. Satta[55], M. Saur[12], D. Savrina[39,38], H. Sazak[7], L. G. Scantlebury Smead[45], A. Scarabotto[8], S. Schael[34], S. Scherl[4], M. Schiller[14], H. Schindler[13], M. Schmelling[87], B. Schmidt[13], S. Schmitt[34], O. Schneider[29], A. Schopper[13], M. Schubiger[1], S. Schulte[29], M. H. Schune[20], R. Schwemmer[13], B. Sciascia[40,13], S. Sellam[5], A. Semennikov[39], M. Senghi Soares[80], A. Sergi[32,89], N. Serra[3], L. Sestini[41], A. Seuthe[12], Y. Shang[75], D. M. Shangase[9], M. Shapkin[24], I. Shchemerov[33], L. Shchutska[29], T. Shears[4], L. Shekhtman[47,96], Z. Shen[75], V. Shevchenko[82], E. B. Shields[51,92], Y. Shimizu[20], E. Shmanin[33], J. D. Shupperd[25], B. G. Siddi[22], R. Silva Coutinho[3], G. Simi[41], S. Simone[61,94], N. Skidmore[16], T. Skwarnicki[25], M. W. Slater[44], I. Slazyk[22,91], J. C. Smallwood[45], J. G. Smeaton[18], A. Smetkina[39], E. Smith[3], M. Smith[31], A. Snoch[1], M. Soares[54], L. Soares Lavra[7], M. D. Sokoloff[11], F. J. P. Soler[14], A. Solovev[17], I. Solovyev[17], F. L. Souza De Almeida[19], B. Souza De Paula[19], B. Spaan[12], E. Spadaro Norella[10], P. Spradlin[14], F. Stagni[13], M. Stahl[11], S. Stahl[13], S. Stanislaus[45], O. Steinkamp[3,33], O. Stenyakin[24], H. Stevens[12], S. Stone[25], M. Straticiuc[60], D. Strekalina[33], F. Suljik[45], J. Sun[37], L. Sun[43], Y. Sun[48], P. Svihra[16], P. N. Swallow[44], K. Swientek[35],

A. Szabelski[76], T. Szumlak[35], M. Szymanski[13], S. Taneja[16], A. R. Tanner[6], M. D. Tat[45], A. Terentev[33], F. Teubert[13], E. Thomas[13], D. J. D. Thompson[44], K. A. Thomson[4], V. Tisserand[7], S. T'Jampens[57], M. Tobin[56], L. Tomassetti[22,91], X. Tong[75], D. Torres Machado[30], D. Y. Tou[8], E. Trifonova[33], C. Trippl[29], G. Tuci[53], A. Tully[29], N. Tuning[1,13], A. Ukleja[76], D. J. Unverzagt[23], E. Ursov[33], A. Usachov[1], A. Ustyuzhanin[26,46], U. Uwer[23], A. Vagner[81], V. Vagnoni[54], A. Valassi[13], G. Valenti[54], N. Vallus Canudas[52], M. van Beuzekom[1], M. Van Dijk[29], E. van Herwijnen[33], C. B. Van Hulse[69], M. van Veghel[65], R. Vazquez Gomez[15], P. Vazquez Regueiro[5], C. Vázquez Sierra[13], S. Vecchi[22], J. J. Velthuis[6], M. Veltri[21,108], A. Venkateswaran[25], M. Veronesi[1], M. Vesterinen[2], D. Vieira[11], M. Vieites Diaz[29], H. Viemann[84], X. Vilasis-Cardona[52], E. Vilella Figueras[4], A. Villa[54], P. Vincent[8], F. C. Volle[20], D. Vom Bruch[27], A. Vorobyev[17], V. Vorobyev[47,96], N. Voropaev[17], K. Vos[66], R. Waldi[23], J. Walsh[36], C. Wang[23], J. Wang[75], J. Wang[56], J. Wang[58], J. Wang[43], M. Wang[58], R. Wang[6], Y. Wang[78], Z. Wang[3], Z. Wang[58], Z. Wang[53], J. A. Ward[2], N. K. Watson[44], S. G. Weber[8], D. Websdale[31], C. Weisser[62], B. D. C. Westhenry[6], D. J. White[16], M. Whitehead[6], A. R. Wiederhold[2], D. Wiedner[12], G. Wilkinson[45], M. Wilkinson[25], I. Williams[18], M. Williams[62], M. R. J. Williams[59], F. F. Wilson[72], W. Wislicki[76], M. Witek[42], L. Witola[23], G. Wormser[20], S. A. Wotton[18], H. Wu[25], K. Wyllie[13], Z. Xiang[53], D. Xiao[78], Y. Xie[78], A. Xu[75], J. Xu[53], L. Xu[58], M. Xu[78], Q. Xu[53], Z. Xu[75], Z. Xu[53], D. Yang[58], S. Yang[53], Y. Yang[53], Z. Yang[75], Z. Yang[48], Y. Yao[25], L. E. Yeomans[4], H. Yin[78], J. Yu[64], X. Yuan[25], O. Yushchenko[24], E. Zaffaroni[29], M. Zavertyaev[87,105], M. Zdybal[42], O. Zenaiev[13], M. Zeng[58], D. Zhang[78], L. Zhang[58], S. Zhang[64], S. Zhang[75], Y. Zhang[75], Y. Zhang[45], A. Zharkova[33], A. Zhelezov[23], Y. Zheng[53], T. Zhou[75], X. Zhou[53], Y. Zhou[53], V. Zhovkovska[20], X. Zhu[58], X. Zhu[78], Z. Zhu[53], V. Zhukov[34,38], J. B. Zonneveld[59], Q. Zou[56], S. Zucchelli[54,93], D. Zuliani[41] and G. Zunica[16]

[1]Nikhef National Institute for Subatomic Physics, Amsterdam, the Netherlands. [2]Department of Physics, University of Warwick, Coventry, UK. [3]Physik-Institut, Universität Zürich, Zurich, Switzerland. [4]Oliver Lodge Laboratory, University of Liverpool, Liverpool, UK. [5]Instituto Galego de Física de Altas Enerxías, Universidade de Santiago de Compostela, Santiago de Compostela, Spain. [6]H.H. Wills Physics Laboratory, University of Bristol, Bristol, UK. [7]Université Clermont Auvergne, CNRS/IN2P3, LPC, Clermont-Ferrand, France. [8]LPNHE, Sorbonne Université, Paris Diderot Sorbonne Paris Cité, CNRS/IN2P3, Paris, France. [9]University of Michigan, Ann Arbor, MI, USA. [10]INFN Sezione di Milano, Milan, Italy. [11]University of Cincinnati, Cincinnati, OH, USA. [12]Fakultät Physik, Technische Universität Dortmund, Dortmund, Germany. [13]European Organization for Nuclear Research, Geneva, Switzerland. [14]School of Physics and Astronomy, University of Glasgow, Glasgow, UK. [15]ICCUB, Universitat de Barcelona, Barcelona, Spain. [16]Department of Physics and Astronomy, University of Manchester, Manchester, UK. [17]Petersburg Nuclear Physics Institute NRC Kurchatov Institute, Gatchina, Russia. [18]Cavendish Laboratory, University of Cambridge, Cambridge, UK. [19]Universidade Federal do Rio de Janeiro, Rio de Janeiro, Brazil. [20]IJCLab, Université Paris-Saclay, CNRS/IN2P3, Orsay, France. [21]INFN Sezione di Firenze, Florence, Italy. [22]INFN Sezione di Ferrara, Ferrara, Italy. [23]Physikalisches Institut, Ruprecht-Karls-Universität Heidelberg, Heidelberg, Germany. [24]Institute for High Energy Physics NRC Kurchatov Institute, Protvino, Russia. [25]Syracuse University, Syracuse, NY, USA. [26]Yandex School of Data Analysis, Moscow, Russia. [27]CPPM, Aix Marseille Univ, CNRS/IN2P3, Marseille, France. [28]Laboratoire Leprince-Ringuet, CNRS/IN2P3, Ecole Polytechnique, Institut Polytechnique de Paris, Palaiseau, France. [29]Institute of Physics, Ecole Polytechnique Fédérale de Lausanne, Lausanne, Switzerland. [30]Centro Brasileiro de Pesquisas Físicas, Rio de Janeiro, Brazil. [31]Imperial College London, London, UK. [32]INFN Sezione di Genova, Genova, Italy. [33]National University of Science and Technology "MISIS", Moscow, Russia. [34]I. Physikalisches Institut, RWTH Aachen University, Aachen, Germany. [35]Faculty of Physics and Applied Computer Science, AGH - University of Science and Technology, Krakov, Poland. [36]INFN Sezione di Pisa, Pisa, Italy. [37]INFN Sezione di Cagliari, Monserrato, Italy. [38]Institute of Nuclear Physics, Moscow State University, Moscow, Russia. [39]Institute of Theoretical and Experimental Physics NRC Kurchatov Institute, Moscow, Russia. [40]INFN Laboratori Nazionali di Frascati, Frascati, Italy. [41]Universita degli Studi di Padova, Universita e INFN, Padova, Padova, Italy. [42]Henryk Niewodniczanski Institute of Nuclear Physics Polish Academy of Sciences, Krakov, Poland. [43]School of Physics and Technology, Wuhan University, Wuhan, China. [44]University of Birmingham, Birmingham, UK. [45]Department of Physics, University of Oxford, Oxford, UK. [46]National Research University Higher School of Economics, Moscow, Russia. [47]Budker Institute of Nuclear Physics, Novosibirsk, Russia. [48]University of Maryland, College Park, MD, USA. [49]Guangdong Provincial Key Laboratory of Nuclear Science, Guangdong-Hong Kong Joint Laboratory of Quantum Matter, Institute of Quantum Matter, South China Normal University, Guangzhou, China. [50]Institute for Nuclear Research of the Russian Academy of Sciences, Moscow, Russia. [51]INFN Sezione di Milano-Bicocca, Milan, Italy. [52]DS4DS, Universitat Ramon Llull, Barcelona, Spain. [53]University of Chinese Academy of Sciences, Beijing, China. [54]INFN Sezione di Bologna, Bologna, Italy. [55]INFN Sezione di Roma Tor Vergata, Rome, Italy. [56]Institute of High Energy Physics, Beijing, China. [57]Univ. Savoie Mont Blanc, CNRS, IN2P3-LAPP, Annecy, France. [58]Center for High Energy Physics, Tsinghua University, Beijing, China. [59]School of Physics and Astronomy, University of Edinburgh, Edinburgh, UK. [60]Horia Hulubei National Institute of Physics and Nuclear Engineering, Bucharest-Magurele, Romania. [61]INFN Sezione di Bari, Bari, Italy. [62]Massachusetts Institute of Technology, Cambridge, MA, USA. [63]Los Alamos National Laboratory, Los Alamos, NM, USA. [64]Physics and Micro Electronic College, Hunan University, Changsha City, China. [65]Van Swinderen Institute, University of Groningen, Groningen, the Netherlands. [66]Universiteit Maastricht, Maastricht, the Netherlands. [67]Eotvos Lorand University, Budapest, Hungary. [68]Institute for Nuclear Research of the National Academy of Sciences, Kyiv, Ukraine. [69]School of Physics, University College Dublin, Dublin, Ireland. [70]NSC Kharkiv Institute of Physics and Technology, Kharkiv, Ukraine. [71]INFN Sezione di Perugia, Perugia, Italy. [72]STFC Rutherford Appleton Laboratory, Didcot, UK. [73]School of Physics and Astronomy, Monash University, Melbourne, Victoria, Australia. [74]Department of Physics and Astronomy, Uppsala University, Uppsala, Sweden. [75]School of Physics State Key Laboratory of Nuclear Physics and Technology, Peking University, Beijing, China. [76]National Center for

Nuclear Research, Warsaw, Poland. [77]Pontifícia Universidade Católica do Rio de Janeiro, Rio de Janeiro, Brazil. [78]Institute of Particle Physics, Central China Normal University, Wuhan, China. [79]Instituto de Fisica Corpuscular, Centro Mixto Universidad de Valencia - CSIC, Valencia, Spain. [80]Nikhef National Institute for Subatomic Physics and VU University Amsterdam, Amsterdam, the Netherlands. [81]National Research Tomsk Polytechnic University, Tomsk, Russia. [82]National Research Centre Kurchatov Institute, Moscow, Russia. [83]INFN Sezione di Roma La Sapienza, Rome, Italy. [84]Institut für Physik, Universität Rostock, Rostock, Germany. [85]Departamento de Fisica, Universidad Nacional de Colombia, Bogota, Colombia. [86]Helmholtz-Institut für Strahlen und Kernphysik, Universität Bonn, Bonn, Germany. [87]Max-Planck-Institut für Kernphysik, Heidelberg, Germany. [88]Present address: Università di Firenze, Florence, Italy. [89]Present address: Università di Genova, Genova, Italy. [90]Present address: Università di Modena e Reggio Emilia, Modena, Italy. [91]Present address: Università di Ferrara, Ferrara, Italy. [92]Present address: Università di Milano Bicocca, Milano, Italy. [93]Present address: Università di Bologna, Bologna, Italy. [94]Present address: Università di Bari, Bari, Italy. [95]Present address: Università di Cagliari, Cagliari, Italy. [96]Present address: Novosibirsk State University, Novosibirsk, Russia. [97]Present address: Università di Roma Tor Vergata, Rome, Italy. [98]Present address: Universidade Federal do Triângulo Mineiro, Uberaba-MG, Brazil. [99]Present address: Hangzhou Institute for Advanced Study, UCAS, Hangzhou, China. [100]Present address: Università di Siena, Siena, Italy. [101]Present address: Università di Padova, Padova, Italy. [102]Present address: Scuola Normale Superiore, Pisa, Italy. [103]Present address: Università degli Studi di Milano, Milano, Italy. [104]Present address: Iligan Institute of Technology, MSU, Iligan, Philippines. [105]Present address: P.N. Lebedev Physical Institute, Russian Academy of Science, Moscow, Russia. [106]Present address: Università di Pisa, Pisa, Italy. [107]Present address: Università della Basilicata, Potenza, Italy. [108]Present address: Università di Urbino, Urbino, Italy. [109]Deceased: S. Eidelman. ✉e-mail: Ivan.Belyaev@cern.ch